Two-Mode Operation in Highly Birefringent Photonic Crystal Fiber

J. Ju, W. Jin, and M. S. Demokan

***Abstract*—A photonic crystal fiber with different air-hole diameters along the orthogonal axes is found to support only the first two modes over a very broad wavelength range (>650 nm). The second-order mode is approximately linearly polarized and has stable-intensity lope positions that do not change in response to environmental disturbances. Strain sensitivity as a function of operating wavelength of a two-mode interferometric sensor made from such a fiber is also investigated.**

***Index Terms*—Finite-element method (FEM), photonic crystal fiber (PCF), two-mode fiber.**

I. Introduction

TWO-MODE optical fibers have been investigated for a number of device applications such as intermodal couplers [1], selective modal filters [2], acoustooptic frequency shifters [3], and strain and temperature sensors [4], [5]. The use of highly elliptical core fibers stabilizes the second-order mode pattern and significantly improves the performance of such devices. The operating wavelength range of such devices is, however, limited due to the limited (∼150 nm) wavelength range available for two-mode operation in elliptical core fibers [6]. In this letter, we propose to use highly birefringent (HB) photonic crystal fibers (PCFs) for two-mode devices. The wavelength range for two-mode operation in PCFs can be much wider than that in elliptical core fibers, and this coupled with other novel wave-guiding properties associated with PCF, could extend significantly the application range of these two-mode devices and open up new possibilities. We report first the modal characteristics of the PCF and then the results of a strain sensor made from such a PCF.

II. Modal Characteristics of PCF

The PCF investigated here is an idealized version of the HB PCF made by Blazephotonics (Fig. 1). The PCF is of an index-guiding type with a solid silica core surrounded by an array of air-hole running along its length. The PCF is characterized by three parameters: the pitch of the air-holes $\Lambda = 4.179\ \mu$m, the diameters of the small diameters $d_1 = 2.239\ \mu$m, and the diameters of the large hole diameter $d_2 = 4.069\ \mu$m. These parameters are estimated from a scanning electron microscope image of the PCF cross section. This PCF is HB because of different air-hole diameters along the orthogonal axes [7]. The modal and birefringent properties of HB PCF can be accurately simulated by using a full-vector finite-element method (FEM) [8], [9]. In this letter, a full-vector FEM is applied to analyze the mode properties of the HB PCF. Because of the symmetry nature of the PCF, only half of the cross section was used during the simulation and a perfect electric or perfect magnetic conductor is applied along the symmetric plane Γ_1. The computational window is chosen beforehand so that the influence of artificial outer boundaries can be neglected. Fig. 2 shows the calculated effective indexes of the first four eigenmodes (the first two modes, each with two eigenpolarization states) and space filling mode (SFM) of the cladding. The effective index of the SFM is evaluated by applying FEM to the elementally piece [9], [10] as shown in Fig. 1.

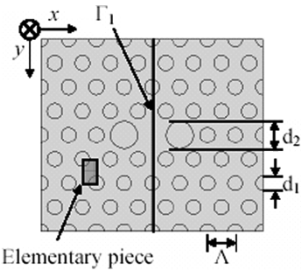

Fig. 1. PCF cross section showing the definition of Λ, d_1, and d_2 and the elementary piece.

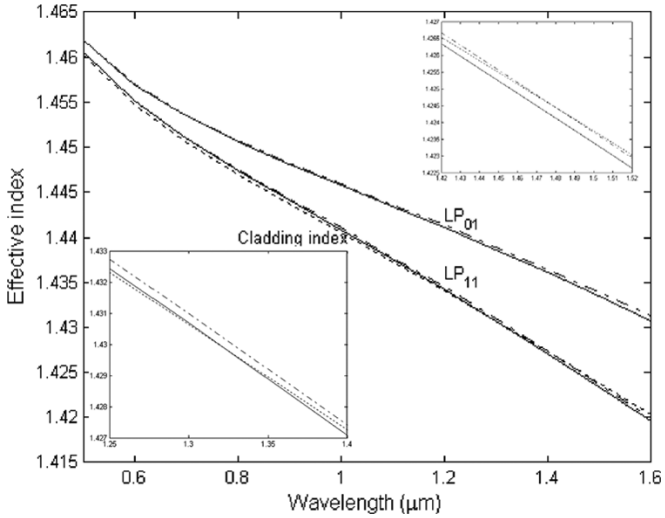

Fig. 2. Dispersion relation (index versus wavelength curve) of the first two guided modes (Dashed–dotted line: x polarization. Solid line: y polarization) and cladding space-filling mode (dotted line).

Simulations show that, over a very wide wavelength range as shown in Fig. 2, the HB PCF supports only four nondegenerate eigenmodes (HE_{11}^x, HE_{11}^y, HE_{21}^x, and HE_{21}^y) with transverse mode field pattern shown in Fig. 3. These modes are approximately linearly polarized and, by analogy to the elliptical core fiber and other asymmetric waveguides, may be labeled as

Manuscript received May 11, 2004; revised July 6, 2004.

The authors are with the Department of Electrical Engineering, the Hong Kong Polytechnic University, Kowloon, Hong Kong (e-mail: jianju.ee@polyu.edu.hk).

Digital Object Identifier 10.1109/LPT.2004.835216

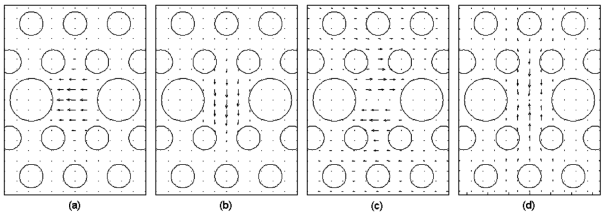

Fig. 3. Transverse electric (TE) field distribution of (a) LP_{01}^{x}, (b) LP_{01}^{y}, (c) LP_{11}^{x} (even), and (d) LP_{11}^{y} (even) modes at 1.3 μm.

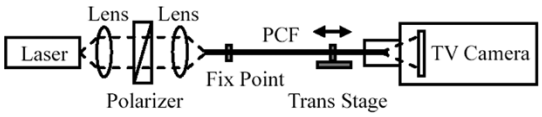

Fig. 4. Experimental setup for measuring the strain sensitivity of two-mode sensor.

LP_{01}^{x}, LP_{01}^{y}, LP_{11}^{x} (even), and LP_{11}^{y} (even), respectively [6], [11]. The superscripts x and y correspond to the x and y polarization modes, respectively. The cutoff wavelengths of LP_{11}^{x} (even) and (even) modes are estimated to be $\sim$1.32 and $\sim$1.48 μm, respectively, corresponding to the intersecting points of their dispersion curves with that of the cladding dispersion as shown in Fig. 2. By applying the V parameter criteria [12] to a nonbirefringent fiber with the same structural parameters (i.e., $\Lambda = 4.179$ μm, $d = 2.239$ μm), the cutoff wavelength of the second modes was found to be $\sim$1.2 μm, corresponding to $V_{\mathrm{PCF}} = \pi$. The discrepancy is due to the introduction of the pair of bigger holes and the results from the dispersion curves are more accurate than that obtained from the V parameter criteria.

It has been found that from wavelengths below the cutoff wavelengths of LP_{11} (even) modes down to 500 nm no higher order modes were found by simulations. The next higher order modes, TE_{01} and TM_{01} modes, corresponding to the two polarization states of the LP_{11} (odd) modes, are completely suppressed because of the nonsymmetrical geometry structure of the HB PCF. This was partially confirmed by our experiments from 650 nm to 1.3 μm as will be described by the next section. Compared with elliptical core fibers that have a two-mode operating range of $\sim$150 nm [6], the PCF studied here possess a remarkable wavelength range of at least 650 nm for the two-mode operation. At wavelength 1550 nm, the HB PCF supports a single mode with two orthogonal polarizations, and the calculated birefringence is 5.38×10^{-4}.

The finding of over 650-nm two-mode operating range in the PCF is significant because it allows for the implementation of very broad-band two-mode fiber devices that are not possible with elliptical core fibers. The choice of proper PCF parameters such as hole size and pitch would allow the two-mode range to be potentially extended into even longer wavelengths of well beyond 1550 nm.

III. Two-Mode Strain Sensor

Sensitivity of a two-mode strain sensor was tested using the setup shown in Fig. 4. Light from a laser was coupled into a piece of HB PCF with an alignment system consisting of a pair of lenses, a polarizer, a fiber holder and a five-dimensional translation stage. An infrared television camera with lens removed is placed near the output of the fiber to monitor the far-field intensity. The PCF has a total length of $\sim$1 m and is epoxy-bounded to a fixed stage and a translation stage. The 50-cm PCF in between the two stages can be axially strained through the computer controlled translation stage.

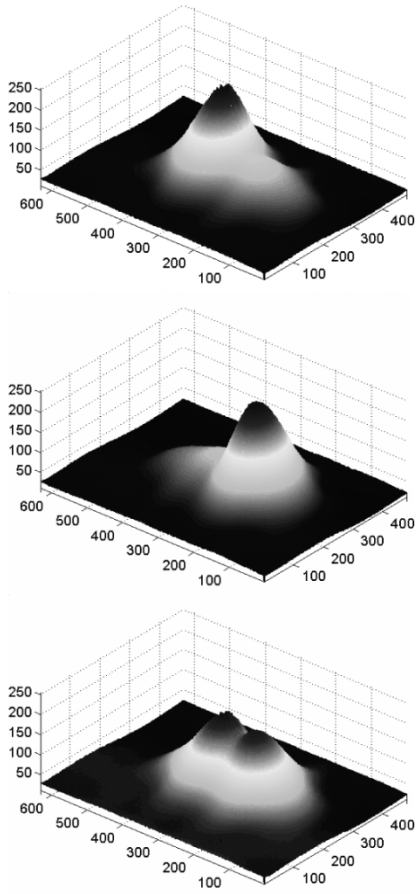

Fig. 5. Measured far-field intensity in two-mode PCF interferometer for phase differences of $0, \pi/2$, and π (from top to bottom). The input polarization is along x direction.

Experiments were conducted at wavelength of 650, 780, 850, 980, 1300, and 1550 nm by using semiconductor lasers. At each wavelength, before applying axial strain to the PCF, the far-field pattern at the fiber output was observed for the lunching conditions were varied. It has been found that at wavelengths from 633 to 1300 nm, the fiber support a fundamental LP_{01} and a second LP_{11} (even) mode. The intensity-lobe orientation of the LP_{11} (even) mode was found stable even when the launching condition is changed. At 1550 nm, only the LP_{01} mode is supported, and no second-order mode was observed. These observations agree with the prediction in Fig. 2.

The strain sensitivity of the two-mode sensor for the five wavelengths from 633 to 1300 nm was then tested. Before each test, the lunching condition was adjusted so that the two modes are launched with approximately equal intensity. This can be achieved by adjusting the offset of the focused incident beam with respect to the axis of the PCF. Taking the operation at 1.3 μm as an example, the focused beam has a diameter of $\sim$3.7 μm, giving a calculated maximum lunching efficiency of 70% for the fundamental LP_{01} mode at zero offset and 23% for the LP_{11} (even) mode at 3.9-μm offset. The intensities of the

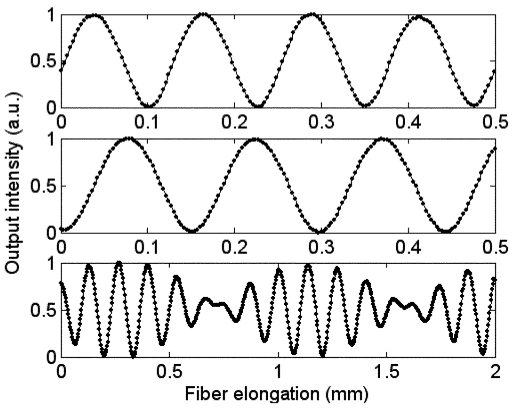

Fig. 6. Experimental results for different launch angles of 0°, 90°, and 45° (from top to bottom).

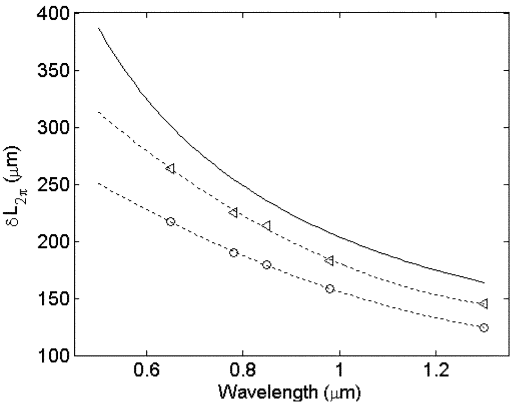

Fig. 7. Measured dependence of $\delta L_{2\pi}$ versus operating wavelength for two polarization states (Circle: x polarization. Triangle: y polarization). Solid line represents the LP_{01} to LP_{11} (even) mode beat length for the unstrained PCF.

two modes are equalized at 3.4-μm offset with lunching efficiency of $\sim$22%. The two modes interfere at the fiber output, resulting in a far-field intensity distribution that varied with the phase difference between the two modes. The operation principle of two-mode PCF interferometer can be easily understood with reference to the recorded intensity distribution of different phases, as shown Fig. 5. In Fig. 5, the evolution of far-field intensity distribution at $\lambda = 1.3$ μm for phase differences of 0, $\pi/2$ and π are shown. For a change of 2π phase difference there will be one complete oscillation. Fig. 6 shows the measured intensity variation at one of the lobes when the PCF was elongated from 0 to 2 mm. The curves from top to bottom correspond to respectively polarizer set to 0°, 90°, and 45°, in respect to the x axis as shown in Fig. 1. At 0° and 90°, the intensity variation is due to the interference of LP_{01} and LP_{11} (even) modes for the x and y polarization, respectively. They are approximately sinusoidal and the elongation $\delta L_{2\pi}$, which is defined as the elongation required for the intensity oscillation to undergo a complete 2π phase shift, is 124.4 and 144.9 μm, respectively. At a launch angle of 45° respective to the principle axis of PCF, the two sets of interference patterns, corresponding to two orthogonal polarizations, are superimposed, resulting in an amplitude-modulated wave, as shown in the lower graph of Fig. 6.

The values of $\delta L_{2\pi}$ for various wavelengths for both polarizations are shown in Fig. 7. Also included in the figure are the calculated beat lengths between the LP_{01} and the LP_{11} (even) modes when the PCF is unstrained (solid line). Contrary to elliptical core two-mode fibers [13], [14], both the modal beat lengths and the elongation needed to produce 2π phase change decrease with the optical wavelength, indicating higher strain sensitivity at longer wavelengths.

IV. Conclusion

The mode properties of an HB PCF are analyzed by using a full-vector FEM. The analyses show that there exists a broad range of wavelength (at least 650 nm) guiding only the fundamental LP_{01} and the second-order LP_{11} (even) modes. This opens the possibilities for building broad-band two-mode fiber devices. A practical two-mode interferometer based on LP_{01} and LP_{11} (even) mode interference is demonstrated for axial strain effect measurement. Unlike two-mode sensors based on elliptical core fibers, the two-mode PCF sensor shows higher sensitivity at longer wavelength. The unique mode properties of HB PCF discussed in this letter are expected to improve the performance of two-mode sensors and devices and to open up new applications in areas such as nonlinear frequency conversion [15].

References

[1] J. N. Blake, B. Y. Kim, and H. J. Shaw, "Fiber-optic modal coupler using periodic microbending," *Opt. Lett.*, vol. 11, pp. 177–179, Mar. 1986.
[2] W. V. Sorin, B. Y. Kim, and H. J. Shaw, "Highly selective evanescent modal filter for two-mode optical fibers," *Opt. Lett.*, vol. 11, pp. 581–583, Sept. 1986.
[3] B. Y. Kim, J. N. Blake, H. E. Engan, and H. J. Shaw, "All-fiber acousto-optic frequency shifter," *Opt. Lett.*, vol. 11, pp. 389–391, 1986.
[4] K. A. Murphy, M. S. Miller, A. M. Vengsarkar, and R. O. Claus, "Elliptical-core two-mode optical-fiber sensor implementation methods," *J. Lightwave Technol.*, vol. 8, pp. 1688–1696, Nov. 1990.
[5] A. M. Vengsarkar, W. C. Michie, L. Jankovic, B. Culshaw, and R. O. Claus, "Fiber-optic dual-technique sensor for simultaneous measurement of strain and temperature," *J. Lightwave Technol.*, vol. 12, pp. 170–177, Jan. 1994.
[6] B. Y. Kim, J. N. Blake, S. Y. Huang, and H. J. Shaw, "Use of highly elliptical core fibers for two-mode fiber devices," *Opt. Lett.*, vol. 12, pp. 729–731, Sept. 1987.
[7] K. Suzuki, H. Kubota, S. Kawanishi, M. Tanaka, and M. Fujita, "High-speed bi-directional polarization division multiplexed optical transmission in ultra low-loss (1.3 dB/km) polarization-maintaining photonic crystal fiber," *Electron. Lett.*, vol. 37, pp. 1399–1401, Nov. 2001.
[8] J. Ju, W. Jin, and M. S. Demokan, "Properties of a highly birefringent photonic crystal fiber," *IEEE Photon. Technol. Lett.*, vol. 15, pp. 1375–1377, Oct. 2001.
[9] M. Koshiba and K. Saitoh, "Finite-element analysis of birefringence and dispersion properties in actual and idealized holey-fiber structures," *App. Opt.*, vol. 42, pp. 6267–6275, Nov. 2003.
[10] T. A. Birks, J. C. Knight, and P. S. J. Russell, "Endlessly single-mode photonic crystal fiber," *Opt. Lett.*, vol. 22, pp. 961–963, July 1997.
[11] A. W. Snyder and X.-H. Zheng, "Optical fibers of arbitrary cross sections," *J. Opt. Soc. Amer. A*, vol. 3, pp. 600–609, May 1986.
[12] N. A. Mortensen, J. R. Folkenberg, M. D. Nielsen, and K. P. Hansen, "Modal cutoff and the V parameter in photonic crystal fiber," *Opt. Lett.*, vol. 28, pp. 1879–1881, Oct. 2003.
[13] J. N. Blake, S. Y. Huang, B. Y. Kim, and H. J. Shaw, "Strain effects on highly elliptical core two-mode fibers," *Opt. Lett.*, vol. 12, pp. 732–734, Sept. 1987.
[14] S. Y. Huang, J. N. Blake, and B. Y. Kim, "Perturbation effects on mode propagation in highly elliptical core two-mode fibers," *J. Lightwave Technol.*, vol. 8, pp. 23–33, Jan. 1990.
[15] L. Provino, J. M. Dudley, H. Maillotte, N. Grossard, R. S. Windeler, and B. J. Eggleton, "Compact broadband continuum source based on microchip laser pumped microstructured fiber," *Electron. Lett.*, vol. 37, pp. 558–560, Apr. 2001.